PHYSICAL REVIEW A VOLUME 39, NUMBER 7 APRIL 1, 1989

Nucleation in the presence of long-range interactions

P. Chandra*
Department of Physics, University of California at Santa Barbara, Santa Barbara, California 93106

(Received 20 June 1988)

We present a theory for nucleation at a first-order phase transition where the mediating forces are long range. We find that the long-range force induces cooperative nucleation and growth processes, and that this feedback mechanism produces a well-defined delay time with a sharp onset in the transformation to the stable phase. Closed-form expressions for the characteristic onset time and width of the transition are developed, in good agreement with numerical and existing experimental results.

I. INTRODUCTION

Unlike droplet nucleation near a liquid-gas critical point, the decay of metastable phases in crystalline materials is strongly affected by the presence of long-range forces.[1] The motivating experiments for our present study are field quenches performed on the ferroelectric barium titanate ($BaTiO_3$) that indicate that nucleation in this material is markedly different from that observed in liquids.[2] $BaTiO_3$ is a classic ferroelectric with a high-temperature phase diagram as shown in Fig. 1(a). The solid line marks a line of first-order cubic (paraelectric) to tetragonal (ferroelectric) transitions, and we note that the phase boundary may be crossed by varying the field or the temperature. In the experiments of McWhan *et al.*[2] a pulsed field brought the system across the phase boundary and let it rest in the spinodal region. The subsequent relaxation was then observed via time-resolved x-ray diffraction.

In the conventional nucleation picture[3] after the field quench the system is viewed as sitting in a free-energy well [Fig. 1(b)]. Initially the system would be in the metastable paraelectric state, but one expects it to decay to the lower ferroelectric state roughly within times on the order of nanoseconds. There would be a smooth transformation to the ordered state with no delay [Fig. 1(c)]. Specifically, as shown in Sec. II C, the conventional Kolmogorov equation predicts a transformation time τ such that

$$\tau=\left[\frac{\pi}{3}I_0\right]^{-1/4}\tau_0\ , \tag{1.1}$$

where I_0 is a Maxwell-Boltzmann factor $e^{-E(R^*)/k_BT}$ (all quantities are defined in Sec. II), $\tau_0=(\Gamma_0 v_0^3)^{-1/4}$, and Γ_0 and v_0 are microscopic nucleation and growth rates, respectively. For the temperature and field quench of interest realistic values[4] of $E(R^*)/k_BT\sim 10$, $\Gamma_0\sim\omega/\xi^3=10^{13}\ \text{sec}^{-1}/(300\ \text{Å})^3$ (ω_0 is the soft phonon frequency and ξ is the correlation length) and $v_0\sim 10^{10}\ \text{Å}\,\text{sec}^{-1}$ yields $\tau_0=4\times10^{-10}$ sec and $\tau=5\times10^{-9}$ sec.

However, when McWhan *et al.*[2] performed their experiments their results were quite surprising; they found that the time dependence of the order parameter (polarization) had a step like shape with a very well-defined delay time that was six orders of magnitude greater than the expected characteristic time scale of the system [Fig. 1(d)]. In a previous paper, Littlewood and I[1] proposed that long-range strain forces, known to be important in $BaTiO_3$ but neglected in the standard droplet model of nucleation,[3,5,6] lead to a time-dependent nucleation rate and a sharp onset in the transformation to the stable phase. In the present study we formulate a more general

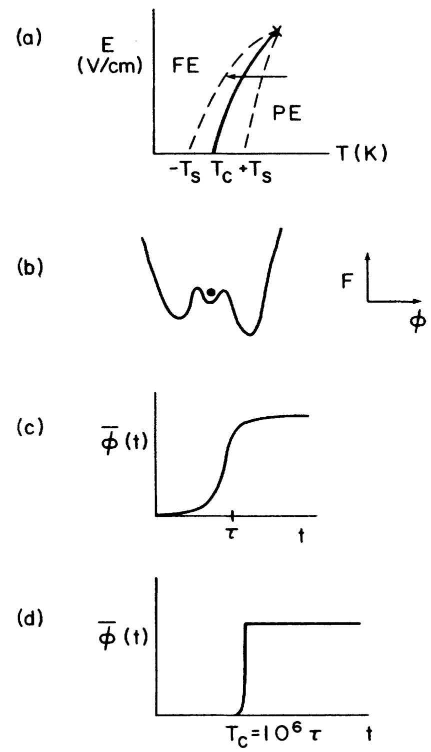

FIG. 1. Schematic views of (a) the high-temperature phase diagram of $BaTiO_3$; the arrow indicates the field quench of McWhan *et al.* (Ref. 2). (b) The system after the field quench. (c) The expected time evolution of $\bar{\phi}$, the system's order parameter, after the field quench. (d) $\bar{\phi}(t)$ vs t found by McWhan *et al.* (Ref. 2).

©1989 The American Physical Society

theory of nucleation and growth that embodies these ideas. In particular, we can now achieve good quantitative agreement with the observed delay time in $BaTiO_3$ and can make a number of predictions for future experiments.

The static properties of the ferroelectric transitions in $BaTiO_3$ are well described by a Landau theory of the coupled order parameters polarization (P) and strain (s).[4] Here we consider only the high-temperature cubic (paraelectric) to tetragonal (ferroelectric) transition in a finite electric field E, and thus take both P and s to be scalars, with s the uniaxial strain (there is negligible volume change at the transition). The free energy per unit volume is written as[4]

$$F(P,s)=\tfrac{1}{2}a(T-T_0)P^2+\tfrac{1}{4}bP^4+\tfrac{1}{6}cP^6 -EP+\tfrac{3}{2}c_e s^2-qsP^2 \ . \tag{1.2}$$

Here T_0 is the Curie temperature, E is the electric field, $c_e=\frac{1}{2}(c_{11}-c_{12})$ is the shear elastic modulus, and $q=c_eQ_{33}$ where Q_{33} is the electrostrictive coefficient. The coefficient b is positive; in the absence of coupling to strain a second-order transition at temperature T_0 would be expected.

Equation (1.2) implies that the onset of polarization will be accompanied by spontaneous strain. If a ferroelectric nucleus is formed inside a paraelectric crystal, there will be an extra cost in energy due to the strain mismatch between the two regions. However, owing to the long-range nature of strain-field interactions, the stress cannot be relieved *only* at the boundary of the two regions, and the energy cost will grow as the volume of the transformed phase. This volume dependence suggests that it is appropriate to approximate the long-range interactions by an infinite model and we write for the total energy

$$F=V_0\sum_i F(P_i,s_i)+\tfrac{1}{2}K(s_i-\bar{s})^2 \ . \tag{1.3}$$

The subscript refers to the individual "nuclei" of volume V_0 (V_0 will be discussed below) and $\bar{s}=(1/N)\sum_i s_i$ is the average strain. The last term in Eq. (1.3) couples the individual strain fields to the average strain in the system; consequently $K\sim c_e$ although specific details depend on the geometry of the individual nucleus.

If we assume that the local strain and polarization are strongly coupled, we may solve for s by setting $\partial F/\partial s=0$ to obtain

$$s=\frac{qP^2}{3c_e} \ . \tag{1.4}$$

We substitute (1.4) into (1.2)

$$F=\tfrac{1}{2}a(T-T_0)P^2+\tfrac{1}{4}\left[b-\tfrac{2}{3}\frac{q^2}{c_e}\right]P^4+\tfrac{1}{6}cP^6-EP \tag{1.5}$$

and note that the coupling to strain renormalizes the fourth-order coefficient in F ($\tilde{b}=b-\frac{2}{3}q^2/c_e$); in the particular case of $BaTiO_3$ the transition is driven first order even within Landau theory.[4] Using the rescaled variable $\phi_i=P_i/P_0(P_o^2=-\tilde{b}/c)$ we express the coarse-grained Helmholtz free energy as

$$F\{\phi\}=f_0\sum_i H(\phi_i)+\tfrac{1}{2}\kappa(\phi_i-\phi_{i+1})^2+\tfrac{1}{4}\gamma(\phi_i^2-\bar{\phi}^2)^2 \ , \tag{1.6a}$$

where

$$H(\phi_i)=\tfrac{1}{2}\tilde{a}\phi^2-\tfrac{1}{4}\phi_i^4+\tfrac{1}{6}\phi_i^6-e\phi_i \tag{1.6b}$$

denotes the free energy for the spatially uniform state. Because the correlation length ξ remains finite at the transition, the system must have a characteristic length scale R^*, determined by competition between volume and surface energies. We have modeled the latter by the gradient term $\frac{1}{2}\kappa(\phi_i-\phi_{i+1})^2$ that corresponds to short-range attractive interactions between nucleating droplets; the scaled coupling constant

$$\gamma=\left[\frac{1}{cP_0^2}\right]\left[\frac{2Kq^2}{3c_e(3c_e+K)}\right]\leq 0.5$$

for the parameters appropriate to $BaTiO_3$.[4,2] The energy scale is set by $\tilde{a}=a(T-T_0)/cP_0^4$ and $f_0=V_0cP_0^6$; here the coarse-graining volume $V_0\sim\xi^3$, ensuring both that the free energy (1.6a) converges rapidly (and is thus meaningful), and that phase separation cannot occur within a single cell (otherwise the details of the nucleation will be lost). In order to get a quantitative feeling for the relevant energy scales involved we note that the local free energy (1.6b) and the gradient term in (1.6a) yield a relation $\epsilon_s=(2/\kappa)\xi^2$ where ϵ_s is the static dielectric constant [$\epsilon_s=\partial^2G/\partial\phi_i^2|_{\phi_i=0}$ where $G(\phi_i)=H(\phi_i)+\frac{1}{2}\kappa(\phi_i-\phi_{i+1})^2$];[4] close to T_0 ($T_0-3\leq T\leq T_0+3$) the static dielectric constant ϵ_s reaches values as high as 10^4 leading to an estimate of $\xi/a_0\sim 50-100$ in this temperature region (a_0 is the lattice spacing). Because of this large correlation length, the energy scale is in the range $f_0/k_BT\sim 3\times 10^3-2\times 10^4$ close to the transition. For finite γ, the free-energy barrier height is proportional to γf_0 ($T\sim T_0$), which is large in comparison with thermal energies; a nucleation treatment is therefore appropriate.

Because we are treating the paraelectric-ferroelectric transition in a finite electric field at fixed temperature, we may simplify the free energy (1.6) before studying its associated dynamics. In particular, the bias field will always select a particular polarization state; the other polarization minimum will play a negligible role in the system's dynamics and can be safely neglected. The appropriate free energy is then

$$\frac{F\{\phi\}}{k_BT}=V_0\sum_i G(\phi_i)+\tfrac{1}{2}\kappa(\phi_i-\phi_{i+1})^2+\tfrac{1}{2}\gamma(\phi-\bar{\phi})^2 \ , \tag{1.7a}$$

$$G(\phi_i)=a(-\tfrac{1}{2}\phi_i^2+\tfrac{1}{4}\phi_i^4)-e\phi_i \ , \tag{1.7b}$$

where $\bar{\phi}=1/N\sum_i\phi_i$ and ϕ_i has been appropriately scaled so that $\bar{\phi}(t\rightarrow-\infty)=-1$ and $\bar{\phi}(t\rightarrow+\infty)=+1$; specifically, we have shifted the variable ϕ_i from its value in Eqs. (1.6). The constant a has *no* temperature dependence; the mapping of (1.6a) to (1.7a) is *only* valid at finite field and constant temperature. We note that in (1.6a) the coupling term $\frac{1}{2}\gamma(\phi_i^2-\bar{\phi}^2)^2$ shifts the system's effective temperature (it renormalizes the ϕ_i^2 coefficient), thereby changing the relative heights of the paraelectric and ferroelectric minima; the term $\frac{1}{2}\gamma(\phi_i-\bar{\phi})^2$ in (1.7) leads to an identical effect.

We can regroup terms in the free energy (1.7) and rewrite it as follows:

$$F=V_0\sum_i \tfrac{1}{2}\kappa(\phi_i-\phi_{i+1})^2+\widetilde{G}(\phi_i)-e\left[1+\frac{\gamma}{e}\bar{\phi}\right]\phi_i\ , \tag{1.8a}$$

where

$$\widetilde{G}(\phi_i)=-\tfrac{1}{2}(a-\gamma)\phi_i^2+\tfrac{1}{4}a\phi_i^4\ . \tag{1.8b}$$

Physically we consider the system to be "trapped" *globally* in a state $\bar{\phi}$; just after the quench $\bar{\phi}=-1$ and *locally* we see that if $\gamma>e$ there will exist not effective bias field and hence no nucleation. Similarly, there will be no transformation for $\gamma>a$; the coefficient of ϕ_i^2 in (1.8b) will now be positive and the system will only have one possible state. This region of infinite metastability ($\gamma>e,a$) is an artifact of an infinite-range model; in finite-range models, the decay time of a metastable state will diverge exponentially with the range of interaction in this region.[7]

The key physics emerging from (1.8) is that the system's effective strain field will depend on the fraction of material transformed. Therefore the critical droplet radius R^*, determined by considering competition between long- and short-range forces, will be a decreasing function of time and will result in time-dependent nucleation and growth rates. The presence of the long-range strain force thus induces a cooperative nucleation and growth process, and we shall see that this feedback mechanism leads to a well-defined delay time and sharp onset in the transformation to the stable phase. Though our study of (1.8) was motivated by experiments on BaTiO$_3$, we believe that this model has more general application in that similar results will be obtained for any double-well model with a long-range coupling term.

The layout of this paper is as follows. In Sec. II we discuss the three self-consistent equations for nucleation, growth, and fraction of the material transformed that will determine the time evolution of the system. Analytic solutions to these equations are then presented in Sec. III, and in particular, we find expressions for the characteristic time and width of the onset curve (see Fig. 2) that are in good agreement with numerical results and with existing experiment. We end with a discussion, and also make suggestions for future work.

II. SELF-CONSISTENT TIME EVOLUTION EQUATIONS

The methods for obtaining expressions for the growth, nucleation, and fraction of the system transformed from a free energy such as (1.8) are well documented;[3] in this section we present the salient features of each derivation but refer the reader to the literature for further details.

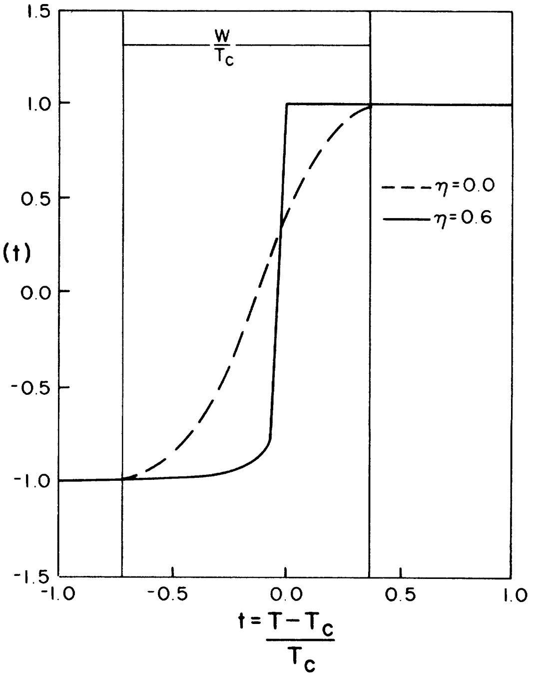

FIG. 2. $\bar{\phi}(t)$ curves for $\eta=0$ and $\eta=0.6$. Here $\bar{\phi}(t=T_c)\equiv1-2e^{-1}$, and W/T_c is shown for the Kolmogorov ($\eta=0$) case.

A. Growth rate

The free energy (1.8) leads to the following evolution equation for a spherical droplet of radius r in $d>1$ dimensions:

$$\frac{1}{\Gamma}\frac{\partial\phi}{\partial t}=\kappa\left[\frac{\partial^2\phi}{\partial r^2}+\frac{(d-1)}{r}\frac{\partial\phi}{\partial r}\right]-\frac{\partial G}{\partial\phi}+e\left[1+\frac{\gamma}{e}\bar{\phi}\right]\ , \tag{2.1}$$

where Γ is a microscopic fluctuation constant. We assume that the droplet retains its shape as it expands, i.e.,

$$\phi(r,t)=\widetilde{\phi}(r-vt)\equiv\widetilde{\phi}(r')\ , \tag{2.2}$$

(2.1) and (2.2) together yield

$$v=\frac{dR}{dt}=\frac{2\Gamma\kappa e(1+\gamma/e)}{\sigma}-\frac{(d-1)\kappa\Gamma}{R}\ , \tag{2.3}$$

where σ is a surface energy

$$\sigma\equiv\kappa\int d^dr\left[\frac{\partial\phi}{\partial r}\right]^2\ . \tag{2.4}$$

Now we may determine the size of the critical radius

$$\frac{dR}{dt}=0\Longrightarrow R^*=\frac{(d-1)\sigma}{2e\left[1+\frac{\gamma}{e}\bar{\phi}\right]}\equiv\frac{R_0^*}{\left[1+\frac{\gamma}{e}\bar{\phi}\right]}\ . \tag{2.5}$$

The crux of the preceding velocity calculation is the use of the traveling wave solution; here we are assuming that the nucleating droplets are spherical. Strictly speaking, the "droplets" in crystalline materials are often cubic or tetragonal (e.g., $BaTiO_3$) but the important macroscopic physics of the system does not lie in the details of this geometry. From (2.5) we see that R^* will depend inversely on the fraction of material transformed $[F(t);\bar{\phi}(t)\equiv 2F(t)-1]$ and this will be a decreasing function of time; initially $\bar{\phi}=-1$ so that $R^*(t\rightarrow-\infty)>R_0^*(t\rightarrow+\infty)$ [see Eq. (2.5)].

B. Nucleation rate

We return to the free energy (1.8) and now discuss the nucleation rate, following closely the treatment of Langer.[8] In order to describe thermally activated processes we must couple the system to a heat bath that drives thermal fluctuations in the system. Then, using well-established statistical methods, an equation of motion, the Fokker-Planck equation, for a distribution-functional $\rho\{\phi\}$ may be derived:

$$\frac{\partial\rho\{\phi\}}{\partial t}=-\int d^3r\frac{\delta J(\mathbf{r})}{\delta\phi(\mathbf{r})}\ , \tag{2.6}$$

where the probability current $J(\mathbf{r})$ is given by

$$J(\mathbf{r})=-D\nabla^2\left[\frac{\delta F}{\delta\phi(\mathbf{r})}\rho+k_BT\frac{\delta\rho}{\delta\phi(\mathbf{r})}\right] \tag{2.7}$$

and D is proportional to the bias field (k_B is Boltzman's constant). The equilibrium solution of (2.6) and (2.7) is

$$\rho_{\rm eq}\{\phi\}\sim\exp(-F\{\phi\}/k_BT)\ . \tag{2.8}$$

Stable and metastable states of the free energy satisfy

$$\frac{\delta F\{\phi\}}{\delta\phi}=-\kappa\nabla^2\phi+\frac{dG}{d\phi}-e\left[1+\frac{\gamma}{e}\bar{\phi}\right]=0\ . \tag{2.9}$$

We can safely assume that local dynamics will be on a time scale significantly faster than that of $\bar{\phi}$; then we can have a metastable state at $\phi=\phi_0$ if

$$\frac{dG}{d\phi_0}=e\left[1+\frac{\gamma}{e}\bar{\phi}\right]\ , \tag{2.10}$$

$$\frac{d^2G}{d\phi_0^2}>0\ . \tag{2.11}$$

A phase transition will occur when the system starts near a metastable state (i.e., $\phi=\phi_0$) and passes through a saddle point of F [also a solution of (2.9)] to a minimum of lower free energy. This saddle point state $F\{\phi_0\}$ represents the free energy of a single localized fluctuation, the critical droplet of the stable phase.

Equations (2.6) and (2.7) may be solved for a steady-state probability current ($\mathbf{J}\neq 0$, $\nabla\cdot\mathbf{J}=0$) flowing across the saddle point. The nucleation rate is then the integrated probability current; such an analysis yields

$$I(t)=Q\Omega_0e^{-\Delta F/k_BT}\ , \tag{2.12}$$

where ΔF is the excess free energy of the droplet

$$\Delta F=F\{\bar{\phi}\}-F\{\phi_0\} \tag{2.13}$$

or, specifically, ΔF is the free energy of a critical droplet of size R^*. Q is a factor that depends on the dynamical properties of the system; in particular, a droplet of size $R=R^*$ will grow like e^{Qt} where

$$Q\sim R^*\ . \tag{2.14}$$

Ω_0 is a statistical volume term that accounts for additional droplet configurational entropy. For the free energy (1.8) the nucleation rate is

$$I(t)=\Gamma_0e^{-F[\phi(R^*)]/k_BT} \tag{2.15}$$

or

$$I(t)=\Gamma_0I_0^{\frac{1}{(1+\gamma/e\phi)^2}}\ , \tag{2.16a}$$

with

$$I_0\equiv\frac{e^{-F[\phi(R_0^*)]/k_BT}}{k_BT} \tag{2.16b}$$

since

$$F\{\phi(R^*)\}\sim R^{*2}\sim\frac{1}{\left[1+\frac{\gamma}{e}\bar{\phi}\right]^2}\ , \tag{2.16c}$$

where we have set $Q\Omega_0\sim\Gamma_0$ (Γ_0 is a microscopic fluctuation rate) since the term in the exponential of (2.15) will dominate $I(t)$ for $I_0<1$.

C. Kolmogorov-Avrami transformation equation

Now that we can calculate $v(t)$ and $I(t)$, we will use Kolmogorov's approach[9] to determine $P(T)$, the probability that the system remains untransformed at time T. An identical expression for $P(T)$ was independently derived by Avrami,[10] though he used a more complicated approach which we will not pursue here. For illustrative purposes let us begin with the simplest case, namely, where both I and v are constant ($I=I_0\Gamma_0$, $R=v_0t$). Following Kolmogorov's arguments[9] let us assume that nucleation occurs at time t such that $0<t<T$; then all nucleation occurring within a volume of radius $R=v_0(T-t)$ will lead to the transformation at $\mathbf{r}=0$ at time T. Therefore we write

$$dP=\prod_{0\leq t\leq T}\ \prod_{0\leq r\leq v_0(T-t)}(1-I_0\Gamma_0d^3r\,dt) \tag{2.17}$$

and

$$P(T)=\exp\left[-\left[I_0\Gamma_0\int_0^T dt'\int_0^{v_0(T-t)}4\pi r'^2dr'\right]\right]\ , \tag{2.18}$$

which yields

$$P(T)=\exp\{-[(\pi/3)I_0\Gamma_0v_0^3T^4]\}\ . \tag{2.19}$$

For time-dependent nucleation and growth rates $I(t)$ and $v(t)$, respectively, (2.18) can be easily generalized to

$$P(T)=\exp\left[-\left[4\pi\int_0^T I(t)dt\int_0^{R(T-t)} r'^2 dr'\right]\right] \qquad (2.20)$$

leading to the simple expression

$$P(T)=\exp\left[-\frac{4\pi}{3}\int_0^T I(t)R^3(T-t)dt\right]. \qquad (2.21)$$

It is important to note that the Kolmogorov treatment neglects the presence of domain walls between coexisting phases; in the absence of such interfacial energies the critical radius is zero. Here we are only interested in nucleated droplets of radius $R > R^*$; strictly speaking, the lower bound of the radial integral in (2.20) should be $R^* > 0$. The inclusion of such a finite R^* leads to no new physics in this model, but only to additional constants and to a rather complicated expression for $P(T)$; we therefore take R^* to be zero in (2.21). In order to maintain consistency, it is important to consider only droplet growth (i.e., not shrinkage) in the expression for $v(t)$, Eq. (2.3).

III. SOLUTION OF THE SELF-CONSISTENT TIME EVOLUTION EQUATIONS

Combining our results from Sec. II, we find that the system's time evolution is determined by the following self-consistent equations:

$$\bar{\phi}(\tilde{T})=1-2\exp\left[-\frac{4\pi}{3}\int_0^{\tilde{T}}\tilde{I}(\tilde{T}-\tilde{t})\tilde{R}^3(\tilde{t})d\tilde{t}\right], \qquad (3.1a)$$

$$\frac{d\tilde{R}}{d\tilde{t}}=(1+\eta\bar{\phi}), \qquad (3.1b)$$

$$\tilde{I}(\tilde{t})=I_0^{(1/1+\eta\bar{\phi})^2}, \qquad (3.1c)$$

where all of the above quantities are dimensionless, $\eta\equiv\gamma/e$, $I_0 \ll 1$ ($I_0 \equiv e^{[-E(R^*)/k_B T]}$) and $\tilde{I}$, $\tilde{R}$, and $\tilde{t}$ have been appropriately scaled by v_0 and Γ_0, the microscopic growth and fluctuation rate, respectively. For convenience we will drop all tildas from this point onwards, but will continue to assume all quantities to be dimensionless. The final form for $\bar{\phi}(T)$ that emerges from this set of equations will be characterized by an onset time T_c and width W (see Fig. 2); here we develop closed-form analytic expressions for both of these quantities and then compare them with numerical results and experiment.

Physically, the presence of a rare thermal fluctuation of length scale R^* [see (2.5) and (2.16)] is required before the system can *begin* to transform from the metastable to the stable phases; if we assume local equilibrium in the metastable state then the system's characteristic time T_c (see Fig. 2) will be essentially determined by a function of the inverse Maxwell-Boltzmann probability $e^{\beta F(R^*)}$. Initially the strain energy cost of nucleating a stable region will be high, and from (2.5) (in dimensionless units) the critical radius R^*

$$R^*=\frac{1}{1+\eta\bar{\phi}} \qquad (3.2)$$

will be large. Because T_c depends exponentially on R^*, it is clear that the characteristic time for the system coupled to the long-range field (finite η) wil be substantially longer than that for the standard Kolmogorov model ($\eta=0$).

Once one critical droplet has transformed to the stable phase there will be a reduction in the effective strain field, and it will become easier for further transformation to occur; specifically, R^* in (3.2) depends inversely on the fraction of material transformed and thus will decrease as a function of time. Therefore at time $T=T_c$ two simultaneous phenomena occur: first, the system's free energy barrier is reduced thereby changing the nucleation rate, and second, the growth rate of the droplet increases. Roughly speaking, the width W is the time interval between the transformation of one droplet and that of the whole system; therefore in order to determine W we must look at the relative changes in $I(t)$ and $v(t)$ [$v(t)\equiv dR/dt$] at $T=T_c$. From (3.1b) and (3.1c),

$$\frac{1}{I(t)}\frac{dI}{dt}=-2(\ln I_0)\eta\frac{d\bar{\phi}}{dt}R^{*3}, \qquad (3.3a)$$

$$\frac{1}{v(t)}\frac{dv}{dt}=\eta\frac{d\bar{\phi}}{dt}R^*, \qquad (3.3b)$$

so that for $I_0 < 1$ ($I_0 = e^{[-E(R^*)/k_B T]}$ so that this is physically reasonable) and finite η the relative increase in $I(t)$ at the transition will be greater than that in $v(t)$ and we expect the nucleation rate to dominate the width W. Intuitively this is not surprising; since $I(t) \sim f(e^{R^*})$ and $v(t) \sim g(R^*)$ it is reasonable that $I(t)$ would be the more affected by changes in the characteristic length scale R^*. We note that for $\eta \rightarrow 0$ or $I_0 \rightarrow 1$, $dI/dt=0$ and W will be determined by the growth rate; we expect this latter width to be greater than that due to nucleation (finite η, $I_0 < 1$) in agreement with numerical results shown in Fig. 3.

From Eq. (3.1) we see that T_c will be determined by the condition

$$\bar{\phi}(T=T_c)=\text{const}, \qquad (3.4a)$$

where we will arbitrarily set $\bar{\phi}(T=T_c)=0$ so that the determining equation for T_c is

$$\ln 2=\frac{4\pi}{3}\int_0^{T_c} I(T-t)R^3(t)dt. \qquad (3.4b)$$

We define the width as

$$\left.\frac{d\bar{\phi}}{dt}\right|_{T=T_c}=\frac{1}{W} \qquad (3.5a)$$

which leads to the expression

$$\frac{1}{W}=\left[2\pi\int_0^{T_c} I(T_c-t)R^2\frac{dR}{dt}dt\right]. \qquad (3.5b)$$

In order to develop a feeling for the quantities W and T_c we go back to Eqs. (3.1) and iterate them numerically (convergence occurs after five steps); the resulting integrands of (3.4b) and (3.5b) are shown in Fig. 4 for both the $\eta=0$ and the $\eta=0.55$ cases ($I_0=0.01$). Let us begin by discussing the characteristic time. In both Figure 4(a) and 4(c) ($\eta=0$ and $\eta=0.55$, respectively) we note that the integrand (3.4b) has the majority of its weight close to the transition; physically, as discussed above, this is because T_c is determined by the characteristic length scale of the system and thus by its growth. T_c will then be determined by the temporal region local to the transition so that we may make the approximations

$$I(T_c-t)\sim I(0) \tag{3.6}$$

and

$$R(t)\sim t \tag{3.7}$$

in (3.4b) to find that

$$T_c=\left[\frac{\pi}{3\ln 2}I_0^{1/(1-\eta)^2}\right]^{-1/4} . \tag{3.8}$$

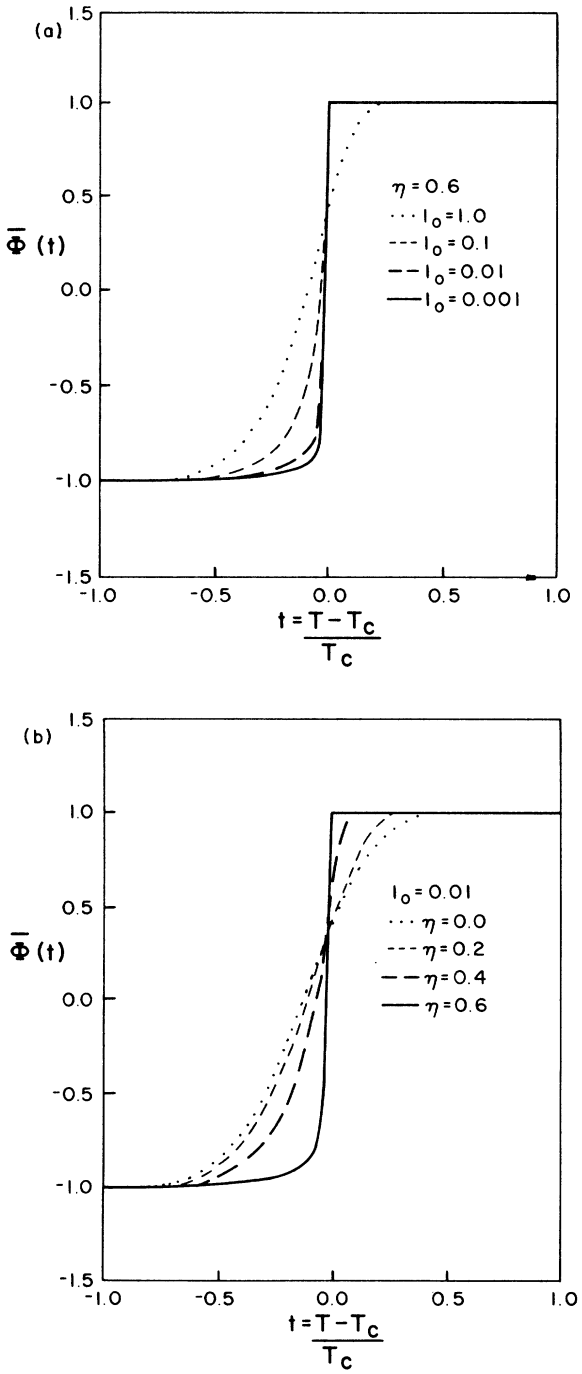

FIG. 3. $\bar{\phi}(t)$ vs t for (a) fixed η and (b) fixed I_0.

Numerical interaction of Eqs. (3.1) yield results in good agreement with (3.8), as shown in Fig. 5. Furthermore, from (3.8) we conclude that for $I_0 \ll 1$

$$\frac{T_c}{\tau}\sim I_0^{-1/4[1/(1-\eta)^2-1]} , \tag{3.9}$$

where τ is the characteristic time scale of the standard Kolmogorov model ($\eta=0$). For the specific case of $BaTiO_3$,[1,2] realistic values of $E(R_0^*)/k_BT=10$ and $\eta=0.6$ yield

$$\frac{T_c}{\tau}\sim 5\times 10^5 , \tag{3.10}$$

which is in quantitative agreement with the experimental results of McWhan *et al.*[2]

Let us now continue and find an expression for the characteristic width W. As shown in Figs. 4(a) and 4(d) the behavior of the appropriate integrand for finite and zero values of η is quite different; as discussed above, for $\eta=0$ W will be dominated by the growth process whereas the nucleation rate $I(t)$ determines W when $\eta\neq 0$. Therefore, in order to calculate the Kolmogorov $\eta=0$ width, we may make the same assumptions as above [namely, (3.6) and (3.7)] and find that

$$\frac{W}{T_c}=\frac{1}{8\ln 2} . \tag{3.11}$$

Physically, since both T_c and W are determined by the same process, it is not surprising that their ratio is a constant.

The width calculation for the finite η case is slightly more complicated; here, as shown in Fig. 4(d), the width is determined by times t just before the onset (i.e., t small). Therefore we may take

$$\frac{dR}{dt}\sim(1-\eta) \tag{3.12}$$

and

$$R^2(t)\sim(1-\eta)^2t^2 \tag{3.13}$$

in (3.5b). We also assume that $I(T_c-t)$ is an exponentially decaying function of (T_c-t)

$$I(T_c-t)=I(T_c)e^{-(T_c-t)/\tau_0} , \tag{3.14}$$

where $\tau_0/W \ll 1$; Fig. 4(b) indicates that this approximation is justified. Expanding $\bar{\phi}(T_c-t)$ about $T-T_c$ and keeping terms to linear order in t/W, we find that

$$\tau_0=\frac{[1+\eta\bar{\phi}(T_c)]^3W}{|\ln I_0|2\eta} , \tag{3.15}$$

which is consistent with (3.14) for $I_0 \ll 1$ and $\eta \to 1$. We then obtain a simple expression for W,

$$W = \left[\frac{2|\ln I_0|}{\pi I_0} \right]^{1/4} \left[\frac{\eta}{1-\eta} \right]^{3/4} . \tag{3.16}$$

For large η and small I_0, W is a very slowly varying function, and is in fact almost a constant. Furthermore, now

$$\left[\frac{W}{T_c} \right] = \left[\frac{2|\ln I_0|}{3 I_0 \ln 2} \right]^{1/4} \left[\frac{\eta}{1-\eta} \right]^{3/4} I_0^{1/4(1-\eta)^2} , \tag{3.17}$$

so that roughly speaking $W/T_c \sim 1/T_c$. Results of numerical iterations of (3) agree with (3.16) for $I_0 \ll 1$, η large as shown in Fig. 6. In Fig. 7 we show more numeri-

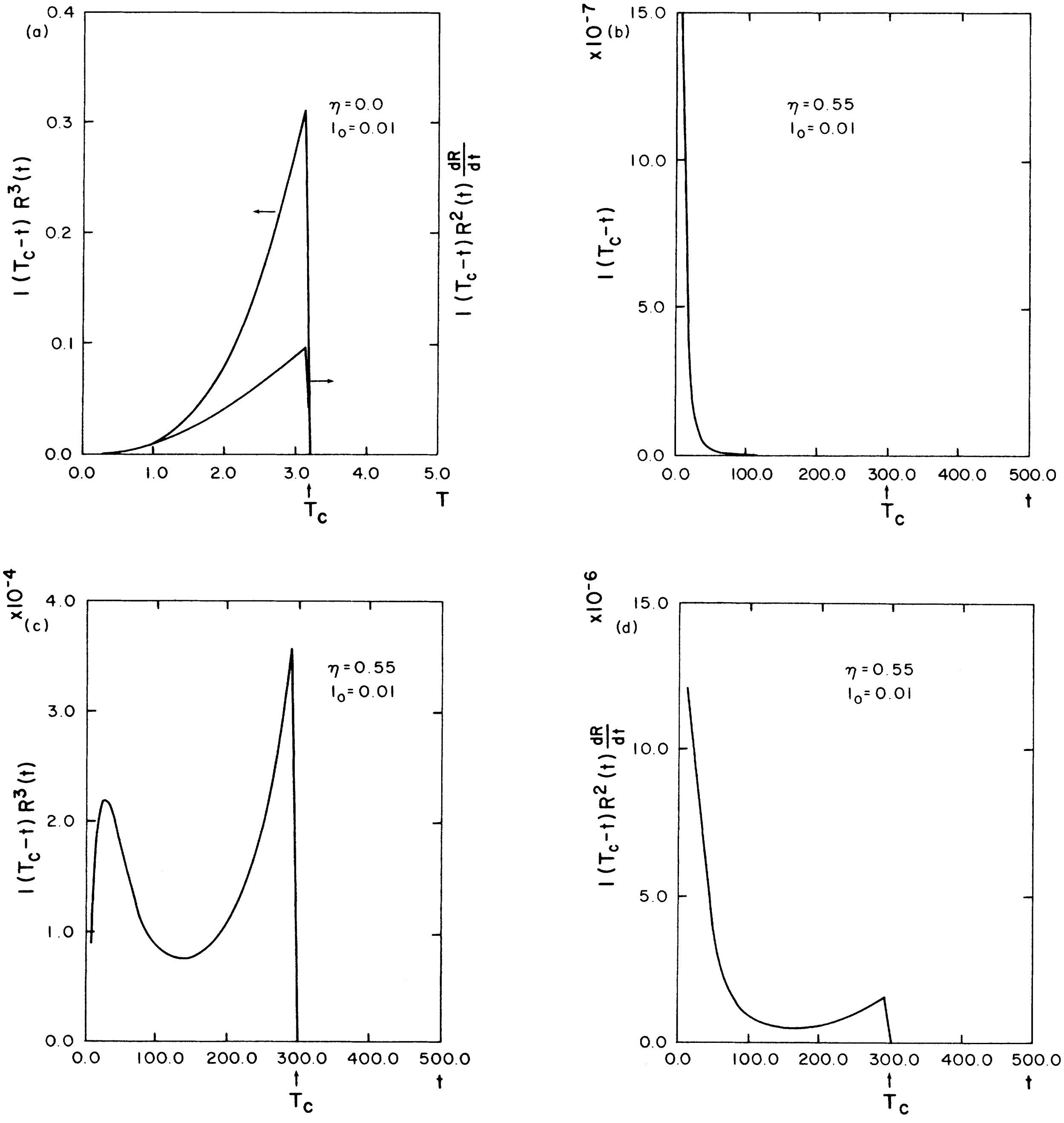

FIG. 4. (a) $I(T_c-t)R^3(t)$ and $I(T_c-t)R^2(t)dR/dt$ for the Kolmogorov ($\eta=0$) model; (b) $I(T_c-t)$; (c) $I(T_c-t)R^3(t)$; and (d) $I(T_c-t)R^2dR/dt$ for $\eta=0.55$ determined by numerical iteration of Eqs. (3.1).

cal results on a $\log_{10}[-\log_{10}(W/T_c)]$ versus $\log_{10}(1-\eta)$ plot; the crossover between Kolmogorov (3.11) and generalized (3.18) behavior is clear as $\eta \rightarrow 1$, $I_0 \ll 1$. Strictly speaking the quantity W/T_c will have yet another crossover in our model; as $\eta \sim 1$, $I_0 \sim 0$ *both* W and T_c will be determined by the nucleation rate, and W/T_c may again be a constant. However, this region of almost infinite metastability is an artifact of our somewhat artificial infinite-range field; here $R^* \rightarrow \infty$ and a discussion appropriate to phase coexistence at a first-order transition is no longer relevant.

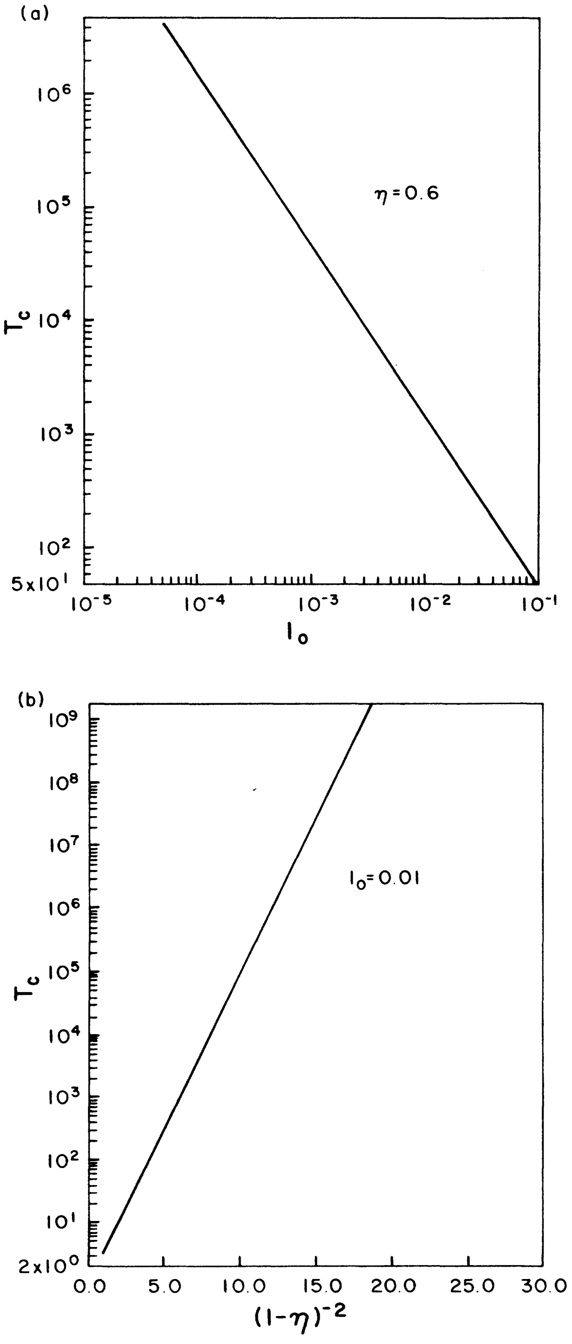

FIG. 5. (a) $\log_{10}T_c$ vs $\log_{10}I_0$ ($\eta=0.6$; slope$=-1.6$) and (b) $\log_{10}T_c$ vs $1/(1-\eta)^2$ ($I_0=0.01$; slope$=0.5$) for results of numerical iteration of Eqs. (3). In both cases the slopes show good agreement with (3.8).

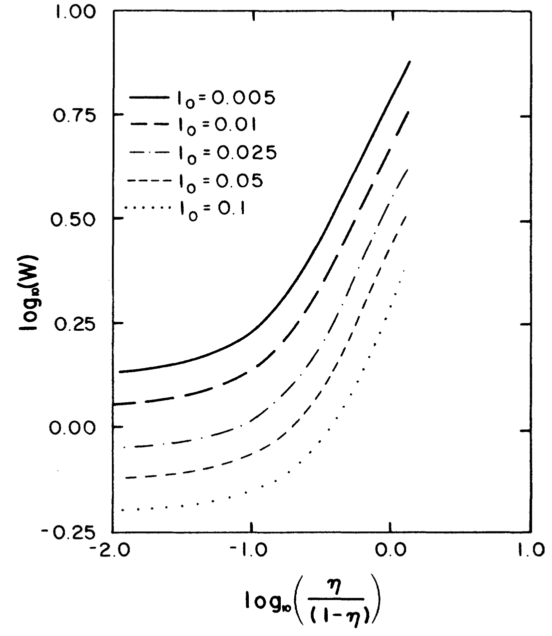

FIG. 6. Numerical iteration of (3) plotted on a $\log_{10}W$ vs $\log_{10}\eta/(1-\eta)$ graph; here the slope is 0.75±0.05 in good agreement with (3.16).

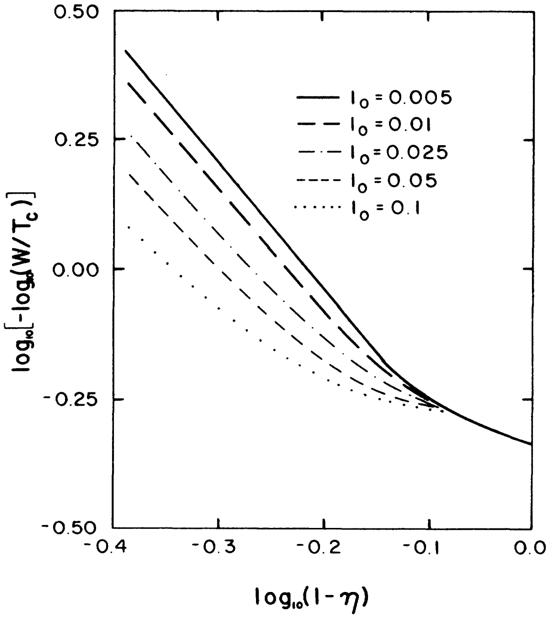

FIG. 7. Numerical iterations of (3) plotted on a $\log_{10}[-\log_{10}(W/T_c)]$ vs $\log_{10}(1-\eta)$ graph; the crossover between Kolmogorov and generalized behavior is clear for $\eta > 0$, $I_0 < 1$ and in each regime the slopes are in good agreement with (3.17) and (3.11), respectively.

IV. DISCUSSION

In conclusion we have presented a theory for nucleation at a first-order phase transition in which the mediating forces are long range. For simplicity we have approximated these long-range interactions by an infinite model, and find that the presence of this mean-field force induces a cooperative nucleation and growth process. In particular, because these infinite-range interactions act to suppress the effect of a bias field, there is a large initial energy cost for creating a stable phase nucleus in the metastable region; however, once one critical droplet has formed, the effective long-range bias field $[e(1+\eta\bar{\phi})]$ "seen" by the material is increased and further transformation becomes significantly easier. The system's characteristic length scale R^*, determined by competition between long- and short-range forces, will therefore depend on the fraction of material transformed and will be a decreasing function of time; this then leads to time-dependent nucleation and growth rates $I(t)$ and $v(t)$, respectively.

Initially the critical radius required for the survival of a stable phase region is very large; this is because the effective bias field seen by the sample is small due to presence of long-range interactions, and a nucleus must overcome large surface energy costs in order to be stable. The system must wait for a rare thermal fluctuation of length scale R^* before it can *begin* to transform, and the expression for T_c, the characteristic time of $\bar{\phi}(T)$, is therefore determined by the growth rate. In Sec. III, following this philosophy, we develop a closed form expression for T_c that agrees well with numerical results (Fig. 5) and with the experiments of McWhan *et al.*[2] for the appropriate parameters. The width of the transition, however, will be determined by the nucleation rate; once one critical droplet as formed the system's free energy barrier will be lowered and the nucleation rate will increase. A closed-form expression for W appears in Sec. III, and it shows good agreement with numerical results. It is important to emphasize that for our generalized (finite η) model W and T_c are determined by *different* physical processes; this is not the case for the standard Kolmogorov picture ($\eta=0$) where both are determined by the growth.

Naturally there remain many open questions and projects for future work. Our closed-form expressions for T_c and W make specific predictions for experiment; unfortunately there is a dearth of data available for comparison. To our knowledge $BaTiO_3$ is the only appropriate experimental system where detailed nucleation studies have been made, and even here only the time delay has been carefully studied. It would be interesting to further explore this phase diagram to explicitly check the crossover behavior of W/T_c. Of course, we would also welcome nucleation experiments on other ferroelectric and magnetoelastic materials, where long-range forces are known to be important.

On the more theoretical side, it might be interesting to study a more sophisticated model where the interactions between nucleating droplets have finite range; specifically one would expect no artificial region of infinite metastability and a probability distribution in the resulting delay times. We should emphasize that the model presented here contains a *scalar* order parameter and it is only valid in a finite bias field *away* from the critical point where a particular stable state will be selected. It would also be interesting to generalize this approach to a model with a continuous order parameter coupled to an infinite-range field; here screening effects will be important and it is not clear whether the resulting long but finite range forces will induce cooperative effects. Such a model may be highly relevant for the inflationary universe scenario,[11] where nucleation theory is used to explain the evolution of the early universe and long-range Higgs forces are thought to be important. In short, though our present study was originally motivated by the simple ferroelectric $BaTiO_3$, we believe that the cooperative nucleation process described here is a far more general phenomena, in that it will be applicable for any double-well model coupled to a long-range field.

ACKNOWLEDGMENTS

The author would like to thank J. S. Langer and P. B. Littlewood for their general support and encouragement throughout the progress of this study. I have also benefited from detailed discussions with P. Coleman, B. Doucot, and R. Rammal. I am grateful to P. W. Anderson and Princeton University for their hospitality when this work was performed, and acknowledge support from the University of California. This work was supported by U.S. Department of Energy Grant No. DE-FG03-84ER45108 and National Science Foundation Grant No. PHY82-17853 supplemented by funds from the National Aeronautics and Space Administration at the University of California at Santa Barbara.

---

[*] Present address: Exxon Research and Engineering Company, Clinton Township, Route 22 East, Annandale NJ 08801.

[1] P. B. Littlewood and P. Chandra, Phys. Rev. Lett. **57**, 2415 (1986).

[2] D. B. McWhan, G. Aeppli, J. P. Remeika, and S. Nelson, J. Phys. C **18**, 1307 (1985); D. A. Neumann, D. B. McWhan, P. B. Littlewood, G. Aeppli, J. P. Remeika, and R. G. Maines, Phys. Rev. B **32**, 1866 (1985).

[3] E.g., J. S. Langer, in *Systems Far From Equilibrium*, Vol. 132 of *Lecture Notes in Physics*, edited by L. Garrido (Springer, Berlin, 1980).

[4] A. F. Devonshire, Philos. Mag. **40**, 1040 (1954); F. Jona and G. Shirane, *Ferroelectric Crystals* (Macmillan, New York, 1962); M. E. Lines and A. M. Glass, *Principles and Applications of Ferroelectrics and Related Materials* (Clarendon, Oxford, 1977).

[5] J. Frenkel, *Kinetic Theory of Liquids* (Dover, New York, 1955).

[6] *Nucleation*, edited by A. C. Zettlemoyer (Dekker, New York,

1969).

[7] R. B. Griffiths, C. Y. Weng, and J. S. Langer, Phys. Rev. B **149**, 301 (1966).

[8] J. S. Langer, Ann. Phys. (N.Y.) **54**, 258 (1969).

[9] A. N. Kolmogorov, Bull. Acad. Sci. USSR Phys. Ser. **3**, 355 (1937).

[10] M. Avrami, J. Chem. Phys. **7**, 1103 (1939).

[11] E.g., *The Very Early Universe,* edited by G. W. Gibbins, S. W. Hawkings, and S. Siklos (Cambridge University Press, Cambridge, 1982), and references therein.